An enhanced Cellular Automata sub-mesh model to study high-density pedestrian crowds

Claudio Feliciani[1], Katsuhiro Nishinari[2,3]

[1] Department of Advanced Interdisciplinary Studies, Graduate School of Engineering, The University of Tokyo, Tokyo 153-8904, Japan
[2] Research Center for Advanced Science and Technology, The University of Tokyo, Tokyo 153-8904, Japan
[3] Department of Aeronautics and Astronautics, Graduate School of Engineering, The University of Tokyo, Tokyo 113-8656, Japan

Abstract. This study presents an alternative mesh system for the floor-field Cellular Automata model which allows reproducing relevant phenomena observed in high density crowds. Sub-mesh positions are created at the edges and at the corners of adjacent cells to increase the mobility in dense crowds. Special rules are introduced to constrain the use of those additional positions and recreate some behavioral features observed in reality. The model was calibrated and validated using empirical data showing good agreement, while similar results could not be obtained using the standard mesh. Finally it was shown that the introduction of the corner sub-mesh position enhances the quality of the results in case of diagonal motion. The model presented here may allow a more accurate investigation of the crowd accidents occurred in the past and prevent a potential re-occurrence in the future.

1 Introduction

Cellular Automata (CA) has been extensively used in the frame of pedestrian dynamics. After the appearance of the first studies at the end of the 20th century [4] there has been an increasing interest in the possibilities given by the use of CA to predict some of the collective phenomena observed in pedestrian crowds. With the evolution of the IT capabilities and the improved computing power, CA models have been used in increasingly larger scenarios with airport terminal or large international events being within the possibilities offered by the system [15]. Additionally, the maximum number of agents has increased, with simulations dealing with hundreds of thousands of agents reported [10] and mid-size simulations running faster than real-time .

Besides performance and technical improvements, recently proposed pedestrian CA models allow to consider complex social structures such as groups [1], which can have a large influence on the overall results. Moreover, models including different walking speeds have been proposed to account, for example, for the situation in which a given fraction of the crowd is composed by elderly [2, 13].

Finally, an anticipation model has been proposed to reproduce the anticipation behavior observed in bidirectional flows [14].

However, while additional features to consider specific aspects of crowds are continuously proposed, the standard mesh used in CA simulations has been almost unchanged since the introduction of the first models. Although some modifications have been proposed throughout the years, such as the real-coded lattice gas model [18] or an hexagonal mesh [19] (both mostly to improve the diagonal motion still being one of weak points of CA), the size of the grid has been almost unchanged, limiting therefore the maximum density allowed in simulations.

Empirical evidence shows that densities up to 8.4 persons m $^{-2}$ [11] are possible in safe controlled experiments and density related to fatal accidents has been estimated as being close to 10 persons m $^{-2}$ [8]. Nonetheless, CA models still typically employ a 0.4 m $\times$ 0.4 m mesh, based on data collected by Weidmann [17]. Some researchers proposed different approaches to increase the maximum density allowed, for example by overlapping pedestrians [3], employing a finer mesh [12, 16] or introducing a force field [9] (which indirectly consider higher densities).

In this study we present a different approach by introducing a sub-mesh model which allows increasing the maximum density achieved in simulations while including some of the behaviors observed in high-density crowds. A similar concept had been introduced in the past [7], but the mesh employed did not allow an accurate reproduction of the diagonal motion. With the model proposed here we aim at allowing a more accurate prediction of high-density crowds by reproducing some typical behavioral patterns and increasing the mobility within the grid to account, for example, for percolation-like phenomena observed in highly congested scenarios [5].

2 Cellular Automata model

In this section the sub-mesh system and the basic transition rules are described and discussed. The fundamental rules of the sub-mesh model (transition probabilities, update sequence, conflict resolution,...) are based on the classic floor-field model (for which a comprehensive description, including some of the particular features used here, is given in [14]). This section will focus on the peculiarities of the sub-mesh concept and shows the differences with similar approaches which appeared in the past.

2.1 Computational mesh

Fig. 1 shows the conventional grid and the sub-mesh grid proposed here. In the conventional approach a square cell is used to approximate the area occupied from a single pedestrian. Pedestrians' motion is therefore simulated by having agents moving from one cell to the next one at each iteration.

If TASEP (Totally Asymmetric Simple Exclusion Process) rules are strictly applied only one pedestrian is allowed per cell and therefore the maximum density reached using conventional grid is 6.25 persons m $^{-2}$ (using a mesh of 0.4

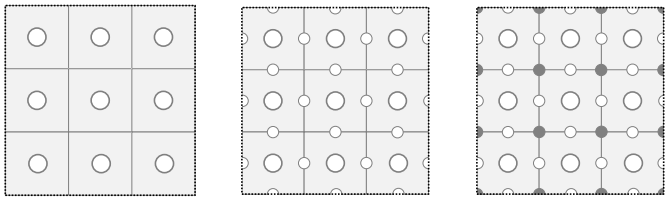

(a) Conventional (b) Sub-mesh (old) (c) Sub-mesh (new)

Fig. 1. Comparison between the conventional and the sub-mesh approach. Sub-mesh locations are indicated with small circles.

m × 0.4 m size). In the sub-mesh approach we decided to add some locations at the boundaries between the cells to increase mobility and allow high-density simulations. In a former approach [7] sub-mesh locations were added between the edges of adjacent cells (Fig. 1(b)). However we found that in case of diagonal geometries such approach may result in largely inaccurate results. To overcome this problem we added some additional positions in the corners as shown in Fig. 1(c). As a consequence, this study will focus on the sub-mesh grid using both edge and corner positions and the following discussion on the model and its rule will focus on the newest approach (Fig. 1(c)).

It is important to notice that while center positions are all equivalent, there exist two types of sub-mesh positions depending on the number of cells which they share. Specifically sub-mesh positions being located at the edges share their location with two adjacent cells, while sub-mesh positions being located at the corners share their location with four neighbor cells. We can therefore assume that pedestrians occupying an edge sub-mesh position are half in one cell and half in the adjacent one. A similar argument can be used for corner pedestrians, but the shared value will be one quarter in this case.

We can now introduce the concept of occupancy which we will use to count the number of pedestrians for each cell. Considering the above arguments the occupancy for each cell (n_{cell}) can be defined as:

$$n_{cell} = n_{center} + \frac{1}{2} \cdot n_{edge} + \frac{1}{4} \cdot n_{corner} \tag{1}$$

where $n_{center} \in \{0, 1\}$, $n_{edge} \in \{0, 1, 2, 3, 4\}$ and $n_{corner} \in \{0, 1, 2, 3, 4\}$ represents the number of pedestrians in the center, the edges and the corners respectively. n_{cell} is 0 when the cell is completely empty and 4 when all the positions are occupied. By using the sub-mesh approach densities 4-times higher than the conventional model (25 m $^{-2}$) are therefore technically possible. However we want to limit the maximum density achieved to values slightly over 10 m $^{-2}$. This can be done by fixing a maximum value of n_{cell}, defined as n_{max} (or maximum occupancy), above which motion to any position of the given cell is not allowed. This approach, besides limiting the maximum density to reasonable values, it allows to recreate a percolation-like behavior because different cells may reach maximum occupancy showing different configurations. From this point of

view the sub-mesh approach differs from a grid-scaling approach, in which at maximum density all cells are equally occupied.

2.2 Transition rules

By only considering the rules described so far the sub-mesh approach would not be much different from an overlapping extension. One of the distinguishing characteristic of the sub-mesh approach lies in the timing rules which apply for the motion to and from the sub-mesh positions.

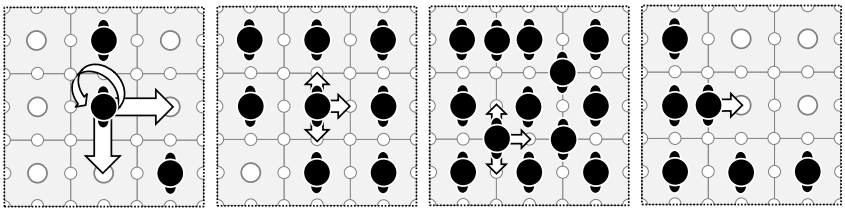

(a) Free-flow (b) Enter crowd (c) Move in crowd (d) Leave crowd

Fig. 2. Different scenarios for a right-walking pedestrian.

Fig. 2 illustrates some typical situations which may be encountered in simulation. Two cases need to be distinguished: motion to a cell center and motion to a sub-mesh position (either edge or corner). The former case will be used to reproduce phenomena observed during free-flow or low-density conditions, while the sub-mesh will be dedicated to high-density considerations. The different rules applying to free-flow and congested motion are summarized as follows:

1. If a neighboring cell center is empty a given pedestrian is allowed to move there the following iteration if maximum occupancy is not exceeded. In other words we can say that a pedestrian being in a situation like the one illustrated in Fig. 2(a) or Fig. 2(d) at the time step t_n can move to the next cell center at t_{n+1} if occupancy n_{cell} for the given cell will not go beyond the maximum occupancy n_{max}. Under low density conditions pedestrians move like in the conventional CA mesh from one cell center to the other.
2. Pedestrians are allowed to move into a sub-mesh position only after having waited a minimum number of t_{wait} iterations (and only if the maximum occupancy will not be exceeded). This rule applies to both pedestrians moving from a cell center and those already being in a sub-mesh position before transition. This rule represents one of the distinguishing points of the sub-mesh approach proposed here. The presence of this rule means that motion to a sub-mesh location or between them is slower compared to center-to-center motion. The motivation hidden behind this rule is that pedestrians do actually move even in congested situations, but their speed is significantly lower and they may have to turn their body to fit between adjacent pedestrians (this last observation is one of the inspirations of the sub-mesh system).

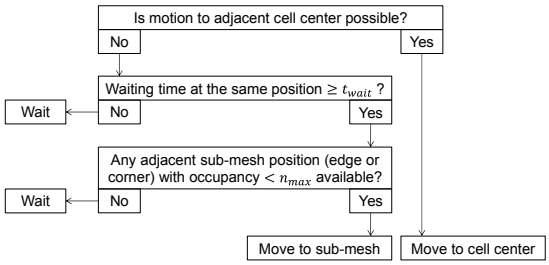

Fig. 3. Transition rules for cell center and sub-mesh positions summarized.

The transition rules described above are schematically summarized in Fig. 3. In addition to the rules introduced earlier we decided to use the exchange probability which allows to avoid head-on collisions by exchanging (or tunneling) the position of two pedestrians being in front of each other and pointing toward opposite directions. To adapt the tunneling method to the sub-mesh approach introduced here we decided to add a penalty to avoid an over-use of this option. For instance a pair of pedestrians walking in different directions may exchange their position if the following two conditions are satisfied:

1. The pair has been waiting in the same position for a time longer than $2 \cdot t_{wait}$.
2. The randomly chosen exchange probability p is smaller or equal than a fixed parameter $p_E \in [0, 1]$. By setting $p_E = 1$ every time that the temporal condition above is satisfied tunneling will occur. Setting $p_E = 0$ will result in no position exchange at all.

The transition probabilities are computed using the standard equations of the floor field model and pedestrians choose their next step according to the transition which has the highest probability. Parallel update is used and in case of a conflict between two pedestrians for the same position, one of the two is chosen with equal probability.

3 Results

3.1 Calibration and validation

The model presented above was calibrated and validated using empirical data resulting from the observation of a bidirectional flow formed by commuters passing a corridor in a subway station (details are given in [6]). Two different scenarios were considered: a normal and a heavily congested case. In the normal case the total flow observed is relatively low and pedestrians simply had to reduce their speed to avoid collisions. In the congested case a deadlock was observed with some of the pedestrians having to stop briefly.

In the simulation, the inflow recorded for each side of the corridor during the observation was used as input, while the output was computed using the

simulation model and later compared with the experimental data as shown in Fig. 4(a) and Fig. 4(b) (total flow is given there). Overall density variation was also compared (see Fig. 4(c) and Fig. 4(d)) and a density map showing the location with highest density was generated at the end of the simulation (see Fig. 4(e) and Fig. 4(f)). 500 simulations were performed for each case.

In general, both the total flow and the density show a satisfactory agreement with the empirical results. Although a comparison is not possible, the density map obtained from simulation reflects the qualitative observation that the densest crowd formed at the right side of the corridor (in the congested case). In particular, using the sub-mesh positions and the waiting time, the double peak observed in the congested case was correctly reproduced.

It is however important to remark that a slightly different set of parameters had to be used. As Table 1 shows, the parameters which had to be adjusted for both cases (normal and congested) generally reflect the partially different attitude observed in the respective situations.

Table 1. Model parameters calibrated using different scenarios. k_S, k_D, k_A and k_W are the values of the static, dynamic, anticipation and wall floor field respectively; α_D and β_D are the diffusion and decay of the dynamic field and d_A is the anticipation distance. Walking velocity is set at 1.4 m $\cdot$ s^{-1}.

Parameter	Normal	Congested	Parameter	Normal	Congested
k_S	8.5	13.0	k_A	8.5	13.0
k_W	0.75		d_A	4	
k_D	6.0		α_D	0.25	
p_E	0.275		β_D	0.25	
n_{max}	2		t_{wait}	1	

3.2 Comparison with the conventional model

To grasp the fundamental differences with the conventional model we performed the congested-case simulation using the standard CA mesh by setting $n_{max} = 1$ and $t_{wait} = 0$. Two different values for p_E were used as given in Fig. 5 which presents the results.

In none of the two cases the double peak (or similar shapes) observed in reality is correctly reproduced. In addition, low values for p_E (generally < 0.10) resulted almost constantly in a complete gridlock as both groups of pedestrians had to stop in front of each other's (simulations were aborted when the given inflow couldn't be reached). This shows that, while the exchange probability has an effect in avoiding head-on collisions, its role is similar to a filter which regulates how much counter-flow is allowed to pass through a crowd. The waiting time and the sub-mesh introduced here create a sort of buffer allowing a temporary increase in density which enhances the permeability of the crowd.

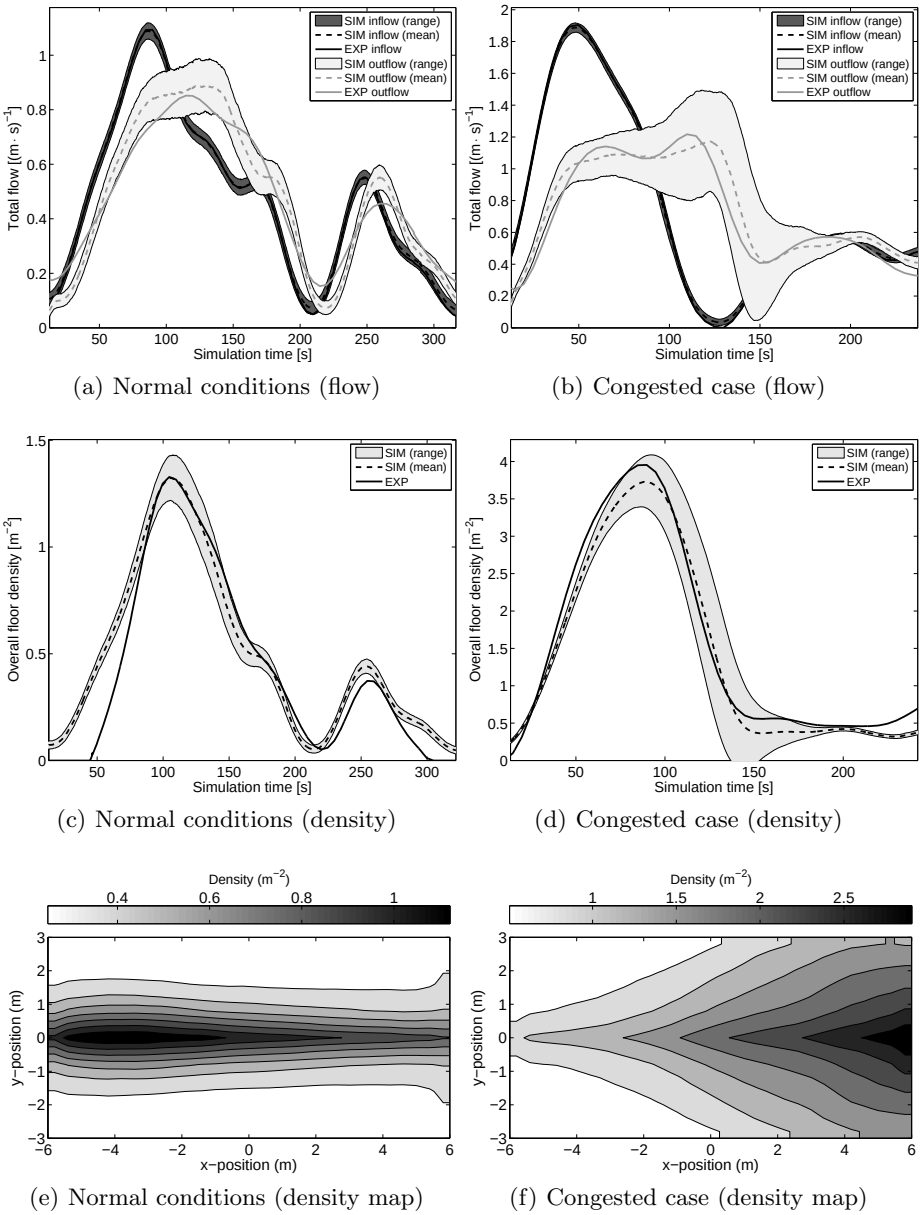

(a) Normal conditions (flow)

(b) Congested case (flow)

(c) Normal conditions (density)

(d) Congested case (density)

(e) Normal conditions (density map)

(f) Congested case (density map)

Fig. 4. Calibration and validation of the model using experimental data. In the graphs representing the flow, dark colors are used for the total inflow and light colors for the total outflow. Thick lines show the experimental result, while dotted line the average simulation result (with the surrounding surface being the variation among the several simulations). In the density maps the effect of the wall floor field is evident; in the congested case a higher density is correctly predicted on the right side. SIM refers to simulation, EXP to experiment.

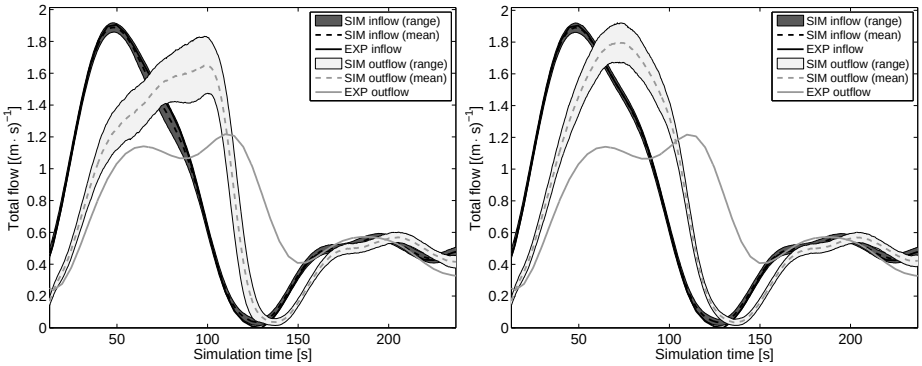

(a) $p_E = 0.15$ (b) $p_E = 0.40$

Fig. 5. Measured and simulated flow in the congested case using the standard mesh ($n_{max} = 1$ and $t_{wait} = 0$). p_E acts as a sort of filter blocking part of the incoming flow. When set too low (in this case about < 0.10) in most of the simulations a complete stop occurred.

3.3 Diagonal motion

Finally we compared the original (old) sub-mesh model (without corner positions) and the improvement proposed here (with corner positions) for the case of a bidirectional flow having different geometrical configurations. We simulated the case of two equally large groups of pedestrians entering a corridor (width 5 m, length 15 m) from both sides. Each group consisted of 200 people and we tested different densities by changing the total flow (from both sides) at the entrance from 1.0 to 2.0 $(\mathrm{m} \cdot \mathrm{s})^{-1}$. To assess the effect of geometrical configuration we changed the angle of the corridor from 0° (horizontal) to 26.56° and finally 45° by keeping the dimensions constant. The parameter-set for the normal case was used and 50 simulations were run for each configuration.
Fig. 6 shows the average density from the beginning (first pedestrian enters corridor) to the end (last pedestrian leaves) of the simulation for the case with a total flow of 2.0 $(\mathrm{m} \cdot \mathrm{s})^{-1}$.

As it can be easily predicted, the highest density is found in the center of the corridor, around 4.0 m^{-2}. In general the density maps are quite similar for the three angles considered, although it appears that in both models the geometry tends to change the distribution of crowd in the center. As it can be observed, in the horizontal case the highest-density region is elongated by reproducing the shape of the corridor. However in the 45° case a more concentric configuration is observed. Similar characteristics were found in the 1.0 $(\mathrm{m} \cdot \mathrm{s})^{-1}$ case which is not reported here.

Concerning the absolute values, it has to be remarked that an higher maximum density is found in the 45° case compared the other two cases. This behavior can be understood considering the group crossing time (the time required by the crowd to completely leave the corridor) given in Table 2.

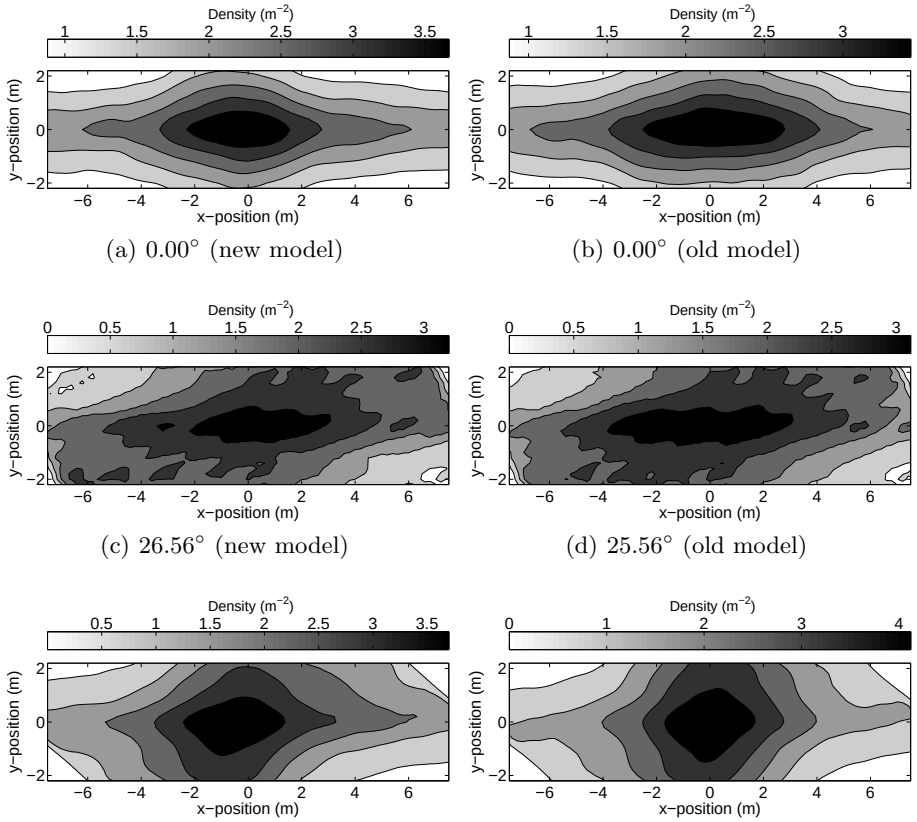

(a) 0.00° (new model) (b) 0.00° (old model)

(c) 26.56° (new model) (d) 25.56° (old model)

(e) 45.00° (new model) (f) 45.00° (old model)

Fig. 6. Average density in the different regions of the corridor for the case with a total flow of 2.0 $(\mathrm{m} \cdot \mathrm{s})^{-1}$. All the cases have been rotated to facilitate visualization and comparison. In the 26.56° case the discrete configuration used in the model results in a light distortion.

Table 2. Group crossing time depending on the total flow and the geometrical configuration used. Clearly the use of the edge location helped improving the diagonal motion in simulations.

Total flow	$1.0\ (\mathrm{m} \cdot \mathrm{s})^{-1}$		$2.0\ (\mathrm{m} \cdot \mathrm{s})^{-1}$	
Model	New	Old	New	Old
0.00°	104.33 s	103.19 s	96.95 s	100.97 s
26.56°	108.69 s	107.16 s	97.43 s	104.08 s
45.00°	109.17 s	108.11 s	102.91 s	122.74 s

As Table 2 shows, while in the low density scenario both models (old and new) perform well when the geometry is changed, for the in 2.0 $(\mathrm{m} \cdot \mathrm{s})^{-1}$ case in the 45° configuration a longer crossing time is required, which creates a denser crowd in the center of the corridor. In the model not using the edge sub-mesh position the effect of the geometry is quite strong and the average crossing time increases of more than 20% because of the change in geometry. The use of the corner position allows reducing this deviation, although an error slightly larger than 5% is still observed.

4 Conclusions

In this study we introduced an alternative grid system to be employed for the simulation of dense crowd scenarios. Additional positions are created between adjacent cells to allow a usage during heavily congested situations. Special rules apply for the use of such positions to limit the maximum density within reasonable limits and mimic some of the behaviors observed in pedestrian crowds. To improve the diagonal motion we added the corner position, which allows an increased mobility under different geometries.

The model was validated using empirical data showing a good agreement, especially when compared with the results obtained by using the conventional approach. To increase the prediction accuracy we had to use a different set of parameters for different situations, but the number of values which had to be adapted was fairly limited. Finally we showed that the addition of the corner sub-mesh position actually helped improving the motion for diagonal geometries, greatly reducing the error resulting from geometrical changes.

Given its peculiarities, in particular concerning the ability to predict percolation-like phenomena, the model presented here may be used, in addition to pedestrian dynamics, in fields such as material engineering (for example to simulate conductive properties in fiber-reinforced materials) or fluid dynamic (for porous medium in particular).

Acknowledgments

This work was financially supported by JSPS KAKENHI Grant Number 25287026 and the Doctoral Student Special Incentives Program (SEUT RA) of the University of Tokyo. In addition the authors would like to thank Tokyo Metro for helping us obtaining the experimental data used for model calibration.

References

1. Bandini, S., Crociani, L., Gorrini, A., Vizzari, G.: An agent-based model of pedestrian dynamics considering groups: A real world case study. In: Intelligent Transportation Systems (ITSC), 2014 IEEE 17th International Conference on. pp. 572–577. IEEE (2014)

2. Bandini, S., Crociani, L., Vizzari, G.: Pedestrian simulation: Considering elderlies in the models and in the simulation results. In: Ambient Assisted Living, pp. 11–21. Springer (2015)
3. Bandini, S., Mondini, M., Vizzari, G.: Modelling negative interactions among pedestrians in high density situations. Transportation research part C: emerging technologies 40, 251–270 (2014)
4. Blue, V., Adler, J.: Emergent fundamental pedestrian flows from cellular automata microsimulation. Transportation Research Record: Journal of the Transportation Research Board 1644, 29–36 (1998)
5. Federici, M.L., Gorrini, A., Manenti, L., Vizzari, G.: An innovative scenario for pedestrian data collection: The observation of an admission test at the university of milano-bicocca. In: Pedestrian and Evacuation Dynamics 2012, pp. 143–150. Springer (2014)
6. Feliciani, C., Nishinari, K.: Phenomenological description of deadlock formation in pedestrian bidirectional flow based on empirical observation. Journal of Statistical Mechanics: Theory and Experiment 2015(10), P10003 (2015)
7. Feliciani, C., Nishinari, K.: An improved cellular automata model to simulate the behavior of high density crowd and validation by experimental data. Physica A: Statistical Mechanics and its Applications 451, 135–148 (2016)
8. Helbing, D., Johansson, A., Al-Abideen, H.Z.: Dynamics of crowd disasters: An empirical study. Physical review E 75(4), 046109 (2007)
9. Henein, C.M., White, T.: Macroscopic effects of microscopic forces between agents in crowd models. Physica A: statistical mechanics and its applications 373, 694–712 (2007)
10. Lämmel, G., Rieser, M., Nagel, K.: Large scale microscopic evacuation simulation. In: Pedestrian and evacuation dynamics 2008, pp. 547–553. Springer (2010)
11. Oberhagemann, D.: Static and dynamic crowd densities at major public events. Tech. Rep. March, Vereinigung zur Förderung des Deutschen Brandschutzes (2012)
12. Sarmady, S., Haron, F., Talib, A.Z.: Simulating crowd movements using fine grid cellular automata. In: Computer Modelling and Simulation (UKSim), 2010 12th International Conference On. pp. 428–433. IEEE (2010)
13. Shimura, K., Ohtsuka, K., Vizzari, G., Nishinari, K., Bandini, S.: Mobility analysis of the aged pedestrians by experiment and simulation. Pattern Recognition Letters 44, 58–63 (2014)
14. Suma, Y., Yanagisawa, D., Nishinari, K.: Anticipation effect in pedestrian dynamics: Modeling and experiments. Physica A: Statistical Mechanics and its Applications 391(1), 248–263 (2012)
15. Szymanezyk, O., Dickinson, P., Duckett, T.: Towards agent-based crowd simulation in airports using games technology. In: Agent and Multi-Agent Systems: Technologies and Applications, pp. 524–533. Springer (2011)
16. Was, J., Lubaś, R.: Towards realistic and effective agent-based models of crowd dynamics. Neurocomputing 146, 199–209 (2014)
17. Weidmann, U.: Transporttechnik der Fussgänger: Transporttechnische Eigenschaften des Fussgängerverkehrs (Literaturauswertung). ETH, IVT (1993)
18. Yamamoto, K., Kokubo, S., Nishinari, K.: Simulation for pedestrian dynamics by real-coded cellular automata (rca). Physica A: Statistical Mechanics and its Applications 379(2), 654–660 (2007)
19. Yanagisawa, D., Nishi, R., Tomoeda, A., Ohtsuka, K., Kimura, A., Suma, Y., Nishinari, K.: Study on efficiency of evacuation with an obstacle on hexagonal cell space. SICE Journal of Control, Measurement, and System Integration 3(6), 395–401 (2010)